Pergamon

Atmospheric Environment Vol. 28, No. 5, pp. 889–897, 1994
Elsevier Science Ltd

1352-2310/94 $6.00 + 0.00

COMPARISON OF A FRACTAL SMOKE OPTICS MODEL WITH LIGHT EXTINCTION MEASUREMENTS

R. A. DOBBINS
Division of Engineering, Brown University, Providence, RI 02912, U.S.A.

and

G. W. MULHOLLAND and N. P. BRYNER
Building and Fire Research Laboratory, National Institute of Standards and Technology, Gaithersburg, MD 20899, U.S.A.

Abstract—Optical cross-sections of carbonaceous aggregates (smoke) formed by combustion sources have been computed based on fractal concepts. Specific extinction depends upon the primary particle size, the structure of the aggregate as represented by the fractal dimension, the fractal prefactor, and the real and imaginary components of the refractive index of the particle material. While the fractal dimension and primary particle diameter are narrowly defined, the refractive index, to which the results are highly sensitive, are disputed. Specific extinction was measured at $\lambda = 450$, 630 and 1000 nm in a smoke-filled chamber with an optical path length of 1.0 m that was equipped to continuously monitor both particle mass and number concentration as the smoke aged during a 90–120 min interval. The smoke was generated by the burning of crude oil in a pool fire. Specific extinction at all three values of λ was found to be constant even though the aggregate number concentration decreases by a factor of 24 owing to cluster–cluster aggregation. The refractive indices at several wavelengths that are required to give agreement with the measured specific extinction are compared with literature values. The inadequacy of Mie theory for spheres in predicting the optical properties of soot aggregates is reiterated.

Key word index: Absorption cross-sections, aging (materials), carbonaceous smoke, fractals, scattering cross-sections, smoke, specific extinction.

NOMENCLATURE

c_m	aggregate mass per unit volume
c_n	aggregate number concentration
d_p	diameter of primary particles composing the aggregate
D	volume equivalent diameter of an aggregate
D_f	fractal or Hausdorff dimension
$E(m)$	function of refractive index given by equation (6)
$E'(m)$	function of refractive index given by equation (10)
$F(m)$	function of refractive index given by equation (6)
$\mathscr{I}_i$	influence coefficient of the ith independent variable
I	transmitted light
I_0	incident light
k	wave number $= 2\pi/\lambda$
k_f	prefactor in the fractal power law
k_λ	monochromatic attenuating coefficient defined by equation (2)
L	optical path length
m	complex refractive index of the soot material
m_i	imaginary portion of the refractive index of the soot material
m_r	real portion of the refractive index of the soot material
n	number of primary particles in an aggregate
n_c	value of n which must be exceeded in order for the aggregate to be large as defined by equation (8)
$\overline{n^1}$	first moment of the aggregate size distribution function which is the average number of primary particles in a population of polydisperse aggregates
$\overline{n^2}$	second moment of the aggregate size distribution function
R_g	radius of gyration of an aggregate
$\overline{R_g^2}$	mean square radius of gyration of a population of polydisperse aggregates
x_i	the ith independent variable
x_p	$\pi d_p/\lambda$
y	the dependent variable, a function of the variable x_i
Σ_{x_i}	probable error divided by the mean of the independent variable x_i
λ	wavelength of light
ρ_p	density of particle material
σ_{abs}	specific absorption for polydisperse aggregates ($m^2 g^{-1}$)
σ_{ext}	specific extinction for polydisperse aggregates ($m^2 g^{-1}$)
σ_{sca}	specific for polydisperse aggregates ($m^2 g^{-1}$)
ω_A	albedo or ratio of scattering to extinction for the aggregate population.

1. INTRODUCTION

The optical properties of carbonaceous smoke have an important bearing on atmospheric visibility because mobile and stationary power plants are sources of this type of particulate pollutant. The optical cross-sections of the smoke produced by diesel engines in particular have been of interest in monitoring the smoke concentration in the engine exhaust pipe. Thus an extensive literature already exists on this topic. In the more recent past there has been recognition that

the smoke produced by combustion processes consists of aggregates which are fractal-like in that they obey the fractal power law relation between the number of primary particles and the radius of gyration of the aggregate. This has resulted in important theoretical understanding that now provides the basis of a more complete description of the optical behavior of these materials.

Atmospheric visibility is determined by the scattering and extinction components of all the molecular and particulate species. In this work we describe measurements of the specific extinction by carbonaceous smoke. The theoretical calculations afford insight into the values of both the extinction and the scattering component and thus to the absorption and the albedo of the smoke aggregates. The theoretical calculations also reveal the input parameters which more strongly influence these optical properties.

2. PROPERTIES OF CARBONACEOUS SOOT AGGREGATES

Properties of the soot material that are relevant to this work are the material density and refractive index. The observations of the density of soot from several sources are listed in Table 1, and these observations are in reasonable agreement. We use the widely quoted value of 1.86 $g\,cm^{-3}$ which is consistent with the data conveyed in Table 1. It is noted that soot emitted from diesel engines in particular may consist of a volatile hydrocarbon component as well as a carbonaceous component. Such soots are expected to have values of both density and refractive index that study we measure the specific extinction coefficient for smoke produced by the burning of crude oil. Benner *et al.* (1990) report that more than 90% of the smoke particle mass produced during the steady burning phase of this same crude oil was carbonaceous.

The consistency of the data for the density of soot is in sharp contrast to the seemingly contradictory information on the complex refractive index. Several summaries of values of the complex refractive index recommended by various investigators are available (Roessler and Faxvog, 1980; Janzen, 1980; Simons and Williams, 1988). Two works of particular interest (Dalzell and Sarofim, 1969; Lee and Tien, 1981) present the results of experiments and provide dispersion models that extend their observations over a significant range of wavelength (see Table 2). While the values of the real portion of the refractive index are disparate in these two works, the imaginary components agree more closely. Both results predict an increase in the imaginary component in the IR spectral regions.

Recent experimental results using TEM analysis of samples from within flames or above smoking flames confirm the use of the fractal-like nature of soot aggregates in describing their complex morphology (Samson *et al.*, 1987; Mulholland *et al.*, 1988; Megaridis and Dobbins, 1990; Köylü and Faeth, 1992, 1993). Simultaneously, fractal concepts were adopted in describing the optical behavior of soot aggregates (Berry and Percival, 1986; Mountain and Mulholland, 1988; Chen *et al.*, 1990; Nelson, 1989a; Dobbins and Megaridis, 1991; Sorensen *et al.*, 1992a). These advances have provided important insight in the description of the optics of aggregate clusters that will be utilized in this work.

Table 1. Measurements of the density of carbonaceous soot

ρ_p ($g\,cm^{-3}$)	Source	Reference
1.95	Acetylene black	Le Chatelier (1926)
1.84	Acetylene black	Rossman and Smith (1943)
1.82–1.85	"Carbon black"	Janzen (1980)
2.05	Acetylene flame	Roessler and Faxvog (1980)
1.9–2.0	Propane flame	Nishida and Mukohava (1983)
1.90	Acetylene flame	J. R. Nelson (1989b)

Table 2. Refractive index of soot at several wavelengths of light

λ(nm)	450	630	1000	Reference
	$1.56+i0.48$	$1.57+i0.44$	$1.65+i0.72$	Dalzell and Sarofim (1969) (Note 1)
	$2.1+i0.40$	$1.9+i0.45$	$1.9+i0.80$	Lee and Tien (1981) (Note 2)

1. From Table 1 of the cited reference for acetylene soot from typical tests on pellets at room temperature. Values of m for $\lambda = 1000$ nm found by interpolation.
2. From fig. 5 of the cited reference for 300 K.

The fractal power law that is applicable to soot aggregates is

$$n = k_f \left(\frac{R_g}{d_p} \right)^{D_f} \quad (1)$$

where R_g is its radius of gyration, d_p is the diameter of the primary particles, D_f is the fractal or Hausdorff dimension, k_f is the prefactor and n is the number of primary particles in the aggregate. Equation (1) applies to soot generated in the laboratory for values of n as small as 10 or less. Such small aggregates cannot display scale similarity that is a fundamental attribute of true mass fractals and are said to be fractal-like aggregates.

Extensive TEM measurements of the value of D_f of hydrocarbon soots sampled from within or above smoking flames are now available (Samson *et al.*, 1987; Mullholland *et al.*, 1988; Megaridis and Dobbins, 1990; Köylü and Faeth, 1992; Sorensen *et al.*, 1992b). These works yield values of D_f in the range of 1.6–1.8, a remarkably narrow range considering the diversity of flame types and fuels in these tests. The values given from samples taken in the plume of turbulent flames for a variety of fuels (Köylü and Faeth, 1992) are also close to 1.75 which is the value employed herein. The TEM-derived values of D_f are supported by observation of the angular distribution of scattering (Zhang *et al.*, 1988; Charalampopoulos and Chang, 1991; Puri *et al.*, 1993) of soot in premixed or diffusion flames. The values of D_f reported from both sampling and optical experiments are in close agreement with computational simulations in which the primary particle size is constant (e.g. Mountain and Mulholland, 1988). This agreement indicates the cluster–cluster aggregation is a dominant growth process of the soot aggregates both within flames where the processes of surface growth and/or surface oxidation simultaneously occur, and in the plume above smoking flames where surface reactions are absent.

The value of prefactor k_f in equation (1) is less well documented. Although additional information on the value of k_f is desired, analysis of experimental optical data (Köylü and Faeth, 1993), and TEM observations (Puri *et al.*, 1993) leads to values that are substantially higher than that found from computational simulations of the cluster–cluster aggregation process. Here the value $k_f = 9.0$ (Puri *et al.*, 1993) is employed. With the values of D_f and k_f available, equation (1) serves as a relationship between the quantities d_p, n and R_g which applies in a statistical sense to the members of a population of aggregates.

Aggregates produced by combustion processes invariably occur in diverse chain lengths or values of n as a result of the cluster–cluster aggregation process. Certain population-averaged quantities are therefore relevant. Thus, the average number of primary particles in an aggregate, $\overline{n^1}$, is the first moment of the aggregate size probability distribution function (PDF). The ratio of the second moment of the PDF to the square of the first moment is a measure of the width of the size PDF that reduces to unity when the aggregate population is monodisperse—consisting of a single value of n with $\overline{n^1} \to n$. Each aggregate has a volume equivalent diameter D that is given by $n^{1/3} d_p$. The mean square radius of gyration $\overline{R_g^2}$ is a population-weighted quantity which is convenient for optical observations. The population-averaged quantities are discussed in more detail elsewhere (Megaridis and Dobbins, 1990; Dobbins and Megaridis, 1991).

3. SPECIFIC EXTINCTION AND ABSORPTION OF CARBONACEOUS AGGREGATES

The optical cross-sections for aggregates have been the subject of a number of recent studies (e.g. Berry and Percival, 1986; Mountain and Mulholland, 1988; Chen *et al.*, 1990; Nelson, 1989a; Dobbins and Megaridis, 1991; Sorensen, 1992a). The results of these studies have been recently compared with one another (Köylü and Faeth, 1992; Sorensen *et al.*, 1992a). The optical cross-sections for polydisperse aggregates have been formulated (Dobbins and Megaridis, 1991) in terms of the relevant moment ratios of the aggregate size PDF and are in agreement with numerical simulations using Rayleigh–Debye theory (Mountain and Mulholland, 1988). This formulation employs moment ratios that often can be estimated in the inevitable absence of detailed information on aggregate size PDF. Many facets of the optical properties of absorbing aggregates remain to be explored in greater detail. These include interactive effects between primary particles, the influence of strong connecting necks between monomers, the optical behavior of very large aggregates, etc.

The light extinction coefficient k_λ for monochromatic light is related to the light transmittance, I/I_0, via Bouguer–Lambert's law

$$\frac{I}{I_0} = e^{-k_\lambda L} \quad (2)$$

where L is the path length. The specific extinction σ_{ext} is obtained by dividing k_λ by the mass concentration, c_m, of smoke aggregates

$$\sigma_{ext} = k_\lambda / c_m. \quad (3)$$

Extinction is the sum of the effects of scattering (redirection of the light) and absorption (conversion of light to heat). The specific absorption can be expressed as

$$\sigma_{abs} = \frac{6\pi E(m)}{\lambda \rho_p}. \quad (4)$$

This expression is based on investigations which lead to the conclusion that the primary particles composing an aggregate act independently in absorption.

The specific scattering σ_{sca} given by (Dobbins and Megaridis, 1991, equation (33) divided by the mass of the aggregate)

$$\sigma_{sca}=\frac{4\pi\overline{n^2}x_p^3F(m)}{\lambda\rho_p\overline{n^1}}\left[1+\frac{4}{3D_f}k^2\overline{R_g^2}\right]^{-D_f/2}. \quad (5)$$

Here $\overline{n^1}$ and $\overline{n^2}$ are the first and the second moments of the aggregate size distribution function, k is the wave number equal to $2\pi/\lambda$, λ is the wavelength of light, the primary particle size number, x_p, is $\pi d_p/\lambda$, and the functions of complex refractive index are defined by

$$E(m)=Im\left(\frac{m^2-1}{m^2+2}\right) \quad F(m)=\left|\frac{m^2-1}{m^2+2}\right|^2. \quad (6)$$

Equations (4) and (5) neglect multiple scattering within the aggregates which has been shown by Berry and Percival (1986) to be a valid approximation for $D_f<2$. The above equations, which apply for polydisperse aggregates, require a relationship between $\overline{n^1}$ and $\overline{R_g^2}$ as discussed elsewhere. An important simplification results when the case of the large monodisperse aggregate is considered. In this instance $\overline{n^2}\to n^2$, $\overline{n^1}\to n$, $\overline{R_g^2}\to R_g^2$, and with $k^2R_g^2\gg 1$ the second term in equation (5) is large compared to unity. The expression for scattering then reduces to

$$\sigma_{sca}=\frac{4\pi x_p^3k_fF(m)}{\lambda\rho_p}\left(\frac{3D_f}{16x_p^2}\right)^{-D_f/2}. \quad (7)$$

The criterion in terms of $n\geqslant n_c$ for the applicability of equation (7) can be found using equations (1) and (5) which yields

$$n_c\approx k_f\left(\frac{3D_f}{4x_p^2}\right)^{-D_f/2}. \quad (8)$$

Combining equations (4) and (7), we find the following expression for the specific extinction

$$\sigma_{ext}=\frac{6\pi E(m)}{\lambda\rho_p}+\frac{4\pi x_p^3k_fF(m)}{\lambda\rho_p}\left(\frac{3D_f}{16x_p^2}\right)^{-D_f/2}. \quad (9)$$

Thus, provided the inequality $n>n_c$ is fulfilled, the expression for σ_{ext} is independent of n and the size PDF. For $d_p=45$ nm and the previously quoted values of k_f and D_f we find $n_c\approx 100$ primary particles per aggregate when the wavelength of light corresponds to the visible spectrum. Since equation (9) is independent of n it applies to a polydisperse population of large aggregates for which $n\geqslant n_c$ for each member. This is found to be the case for the experiments described below. Examination of equation (9) shows that the scattering contribution to the specific extinction varies directly with k_f, $x_p^{3-D_f}$ and with $F(m)$. On the other hand, the specific absorption is proportional to $E(m)$ and is independent of n and the fractal attributes, k_f and D_f.

From equations (7) and (9) the aggregate albedo ω_A, which is the ratio of specific scattering to specific extinction is calculated. For large aggregates, $n\geqslant n_c$, the value of albedo is independent of n but does depend on both $E(m)$ and $F(m)$.

For larger primary particles or shorter wavelengths the absorption cross-section is improved by the use of a second order correction in x_p. In this case $E(m)$ in equations (4) and (9) is replaced by $E'(m)$ which can be found to be (Bohren and Huffman, 1983)

$$E'(m)=E(m)+Im\left[\frac{x_p^2}{15}\left(\frac{m^2-1}{m^2+2}\right)^2\left(\frac{m^4+27m^2+38}{2m^2+3}\right)\right]. \quad (10)$$

Equation (4) for absorption is applicable for $\pi d_p/\lambda\leqslant 0.1$. The use of $E'(m)$ in lieu of $E(m)$ extends the usefulness of equation (4) to the values of $\pi d_p/\lambda\approx 0.5$. This improvement is employed in calculations of σ_{ext}, σ_{abs} and ω_A quoted below where the wavelengths considered extend to the violet region of the visible spectrum. (The values of σ_{abs}, σ_{sca} and σ_{ext} given by equations (4), (5) and (9) are expressed in the customary units of $m^2\,g^{-1}$ if a factor of 1000 is included in their numerators, λ is in nm, and ρ_p is in $g\,cm^{-3}$.)

4. SENSITIVITY ANALYSIS

A sensitivity analysis can be performed to determine the extent to which the several variables influence the specific extinction and absorption. Thus if $y=f(x_i)$ for $i=1$ to n independent variables, then the total error ε_y is given by

$$\varepsilon_y=\left[\sum_i\{\mathscr{I}_i^2\varepsilon_{x_i}^2\}\right]^{1/2} \quad (11)$$

where the influence coefficients $\mathscr{I}_i$ are denoted by

$$\mathscr{I}_i=\frac{\partial(\ln y)}{\partial(\ln x_i)} \quad (12)$$

and ε_{x_i} represents the probable error divided by the mean for the several independent variables. The influence coefficients $\mathscr{I}_i$ for y equal to σ_{abs}, σ_{ext} and ω_A given in Table 3 were evaluated numerically for the case of $\lambda=630$ nm with the values of the other inputs as stated. It is apparent that both σ_{abs} and σ_{ext} are sensitive to the real component of the refractive index m_r and the imaginary part m_i as well. The

Table 3. Influence coefficients $\mathscr{I}_{x_i}$ for error propogation in determination of σ_{abs}, σ_{ext} and ω_A (based on $\lambda=630$ nm, $d_p=45$ nm, $D_f=1.75$, $k_f=9.0$, $m=1.55+i0.78$)

x_i	$\mathscr{I}_{x_i}$, $y=\sigma_{abs}$	$\mathscr{I}_{x_i}$, $y=\sigma_{ext}$	$\mathscr{I}_{x_i}$, $y=\omega_A$
m_r	−1.22	−0.78	+1.62
m_i	+0.88	+1.01	+0.40
d_p	+0.08	+0.36	+0.49
D_f	0	+0.67	+2.10
k_f	0	+0.24	+0.74

opposite signs of these coefficients imply, for example, that when m_r is increased incrementally the value of σ_{ext} is reduced since $\mathcal{I}_{m_i}$ is negative. On the other hand, if m_i is increased incrementally, then the value of σ_{ext} would be increased since $\mathcal{I}_{m_r}$ is positive. The quantities $\mathcal{I}_{D_f}$ and $\mathcal{I}_{k_f}$ influence only σ_{ext} but not σ_{abs}. The value of σ_{abs} depends weakly on d_p through the second order term given by equation (10). From the values of $\mathcal{I}_{x_i}$ for σ_{ext} given in Table 3 we find the uncertainty ε_{ext} of σ_{ext} would equal $\pm 7.5\%$ if all five input quantities were uncertain to $\pm 5\%$.

5. THE MEASUREMENT OF SPECIFIC EXTINCTION BY AGING SMOKE

The fuel used in this study was Alberta Sweet crude oil with a boiling point range during distillation from 37 to 350 °C, density at 20 °C, 0.84 g cm^{-3}, and flash point, 7 °C. The crude oil was burned in a 0.6 m-diameter pan positioned under a 2.4 × 2.4 m collection hood. A propane torch was used to ignite the 1 cm thick layer of oil floating on about 4 cm of water. A "tripper" orifice plate at the base of the exhaust stack ensured good mixing five diameters downstream where the smoke was drawn into the aging chamber.

The chamber is a 1 m^3 aluminum box which has been lined with stainless steel to reduce corrosion from the hot combustion gases. Forty-eight mica resistance strip heaters are attached to the aluminum wall which evenly distribute the heat for wall temperatures up to 150 °C. In our study, the wall temperature was either at ambient conditions or near 100 °C, which is approximately equal to the exhaust duct temperature. An exhaust fan draws the smoke through the chamber at a flow of 0.13 m^3 s^{-1}. The chamber is connected to the exhaust stack via 10 cm diameter stainless steel tubing (Fig. 1). After the chamber is filled, two stainless steel butterfly valves, one on the inlet and one on the outlet, are simultaneously closed to capture a 1 m^3 sample. Ports at opposite ends of the chamber allow use of a three wavelength photometer for light extinction measurements.

The photometer, similar to the one previously described (Cashdollar *et al.*, 1979), consists of a white light source, two beam splitters, three interference filters, and three photodiodes as illustrated in Fig. 1. The path length through the smoke is 1.0 m. To minimize forward scattered light from reaching the detector, a 1 cm diameter 20 cm long tube is positioned just outside the chamber before the detector assembly. Purged air is used to prevent smoke deposition on the optical components. The interference filters allow measurement of the light extinction coefficient at 450, 630, and 1000 nm. The ratio of the transmitted to incident light was about 0.35 for $\lambda = 450$ nm, 0.45 for $\lambda = 630$ nm, and 0.60 at $\lambda = 1000$ nm for the chamber filled with smoke.

The accuracy of the monochromatic attenuation coefficient, k_λ, can be affected by both smoke deposition on the optical components and by a drift in the photometer light intensity measurement. The combined impact of both of these effects was determined by measuring the light intensity at each of three wavelengths before collecting smoke and then at the end of the experiment after the smoke had been cleared from the chamber. The value of k_λ was computed based on using each of these values for I_0 in equation (2), and then the fractional difference,

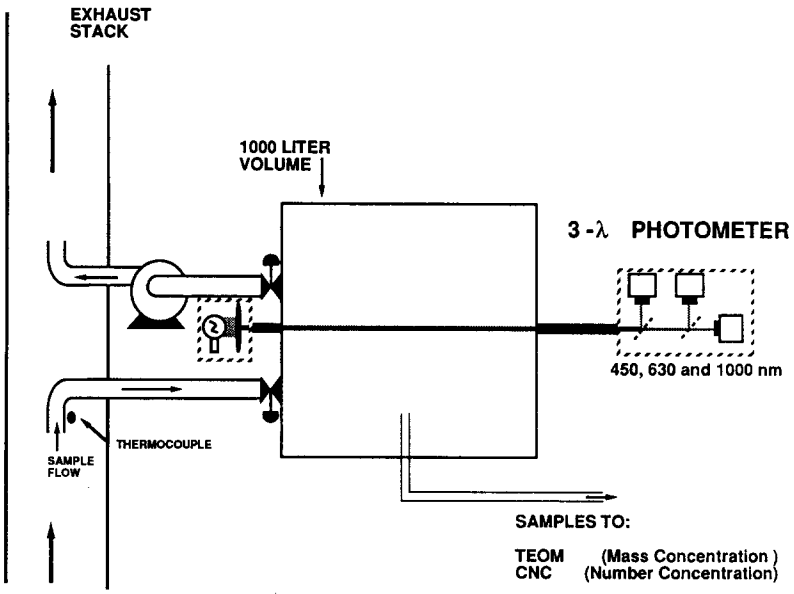

Fig. 1. Schematic diagram of smoke aging apparatus with three wavelength photometer.

$\Delta k_\lambda/k_\lambda$, was computed for each wavelength for three experiments. The average fractional change was 0.0122 ± 0.008 indicating that smoke deposition and the drift in light intensity had a minor effect on the measured values of k_λ.

In order to compute the mass specific light extinction coefficient, the mass concentration of the c_m smoke in the chamber was determined with a Tapered Element Oscillating Microbalance (TEOM). A continuous flow condensation nucleus counter (CNC) was used to monitor the number concentration c_n during an aging experiment. Because of the high initial number concentration, the smoke was diluted about 50-fold before entering the nucleus counter. The initial mass concentration of the smoke was typically on the order of $100\,\mathrm{mg\,m^{-3}}$ and the concentration decreased by about a factor of two over a 2 h aging experiment as a result of particle sedimentation and wall loss. The filtered air introduced to balance the air being withdrawn for the TEOM and CNC is less than 5% of the chamber volume and is not corrected for in these experiments.

In Fig. 2 we present a graph of the measured mass c_m and number concentration c_n, and σ_{ext} at $\lambda = 1000$ nm vs time for one test of 90 min duration. These results show that the mass concentration decreases in that time interval by 30% owing to gravitational settling or diffusion to the chamber walls. On the other hand, the aggregate number concentration decreases by a factor of 24 caused mainly by cluster–cluster aggregation. The specific extinction at $\lambda = 1000$ nm remains essentially constant despite the dramatic change in c_n. The values of σ_{ext} are in general agreement with several that have appeared in the literature as summarized in Table 4. There the low values (Bruce *et al.*, 1991) may be influenced by the presence of a volatile component. The values of σ_{ext} obtained from a butane flame (Colbeck *et al.*, 1989) are noted to be higher than most others for reasons that are not clear at this time.

Table 4. Selected measurements of specific extinction of carbonaceous soot aggregates

λ (nm)	σ_{ext} (m^2g^{-1})	Source	Reference
514.5	9.8 ± 0.8	(a)	Roessler and Faxvog (1980)
514.5	8.9 ± 0.5	(b)	Japar and Szkarlat (1981)
555	7.9 ± 4.5	(c)	Scherrer *et al.* (1982)
632	10–12	(d)	Colbeck *et al.* (1989)
488	10	(e)	Patterson *et al.* (1991)
633	8		
488	6.97 ± 0.31	(f)	Bruce *et al.* (1991)
1060	3.59 ± 0.16		
450	9.7 ± 1.5	(g)	Present work (1993)
630	7.8 ± 1.2		
1000	5.1 ± 0.8		

(a) Acetylene smoke.
(b) Graphitic component of diesel smoke.
(c) Diesel smoke.
(d) Liquefied petroleum gas, mainly butane.
(e) Hydrocarbon fuels and plastics.
(f) Diesel fuel burning on wick supported flame.
(g) Crude oil pool fire.

6. COMPARISON OF THEORY AND EXPERIMENTS

Based on the measured c_m and c_n given in Fig. 2, the density of soot material, and using an estimated primary particle size of $d_p = 45$ nm, we calculate the initial average number of primary particles per aggregate $\overline{n^1}$ to be 190 and the final value to be 4400. The experimental observations thus indicate that the specific extinction remains constant during the time in-

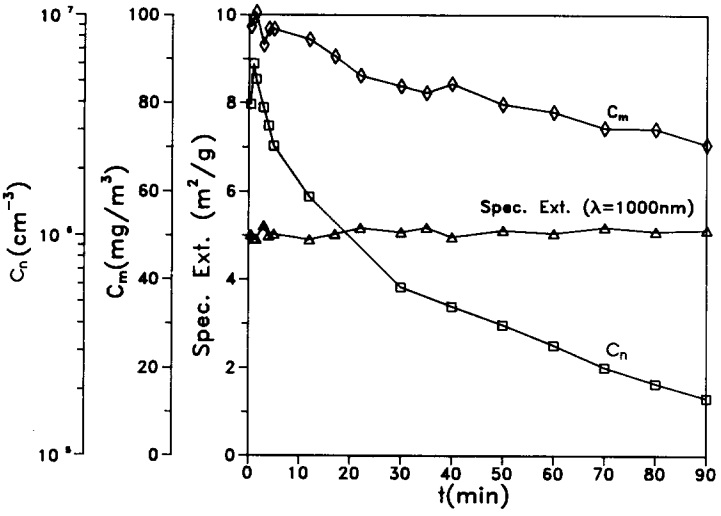

Fig. 2. Soot mass concentration, number concentration and specific extinction vs time.

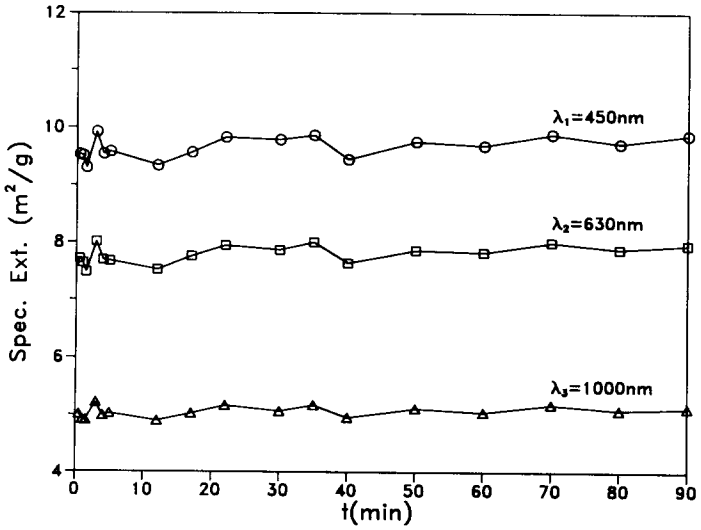

Fig. 3. Specific extinction at three wavelengths vs time.

Table 5. Values of m that give agreement between experimental (exp) values of σ_{ext} and theoretical (th) values with σ_{sca}, σ_{abs}, and ω_A

λ (nm)	σ_{ext}(exp) ($m^2 g^{-1}$)	m	σ_{ext}(th) ($m^2 g^{-1}$)	σ_{sca}(th) ($m^2 g^{-1}$)	σ_{abs}(th) ($m^2 g^{-1}$)	ω_A(th) (%)
450	9.7	$1.55+i0.609$	9.70	2.81	6.89	28.9
630	7.8	$1.55+i0.780$	7.80	1.78	6.00	23.1
1000	5.1	$1.55+i0.929$	5.10	0.82	4.28	16.1

terval that the average aggregate chain size $\overline{n^1}$ increases by a factor of 24. The constancy of σ_{ext} is confirmed in Fig. 3 where values of σ_{ext} for all three wavelengths are presented and are shown to be remarkably constant with time. These results are in agreement with the theoretical predictions for the large aggregates that are observed in these experiments. The results also agree with a number of experiments in which an exponential dependence of transmission is observed over a wide range of particle concentration even for widely varying size distribution—a prediction that would not be supported by Mie theory based on the volume equivalent diameter of the aggregates.

In Table 5 we list the values of refractive index that yield agreement between the measured and the observed values of specific extinction. In this calculation $D_f = 1.75$, $k_f = 9.0$, $\rho_p = 1.86\ g\,cm^{-3}$ and $d_p = 45$ nm. The latter number is used based on sizes shown in a micrograph of soot aggregates formed in a crude oil pool fire conducted at NIST before the current tests. The values of refractive index for soot that are given in Table 4 are closer to the values of refractive index reported (Dalzell and Sarofim, 1969) although the imaginary component is somewhat larger than these authors found in their work. Uncertainties in the quantities that were not measured may possibly account for this discrepancy. For example, the uncertainty analysis indicates that specific extinction is moderately sensitive to the quantities d_p, D_f and k_f. Thus an underestimation of these quantities by 10% would reduce the imaginary portion of the refractive index m_i that is required for agreement between theory and experiment by about 10%.

The albedos that are yielded by the theory for the best fit values of m are in general agreement with the limited observations in the existing literature. These values range from 0.16 (Scherrer *et al.*, 1982), 0.25–0.30 (Colbeck *et al.*, 1989), to 0.34% (Bruce *et al.*, 1991).

The values of refractive index that give agreement are not uniquely determined by solely matching the specific extinction. Thus equally good agreement is found if $m = 1.90 + i0.949$ when an albedo of 32.6% is recovered for $\lambda = 630$ nm. The value of m_r is then in agreement with Lee and Tien (1981) but the imaginary portion is much larger. To resolve these uncertainties it is apparent that both the specific extinction and the specific absorption must be measured and better estimates of d_p and D_f are also needed.

In Fig. 4 σ_{ext} is plotted vs the number of primary particles per aggregate from equations (1), (4) and (5) for the case of monodisperse aggregates with $\lambda = 630$ nm, $d_p = 45$ nm, $D_f = 1.75$, and $m = 1.55 + i0.78$.

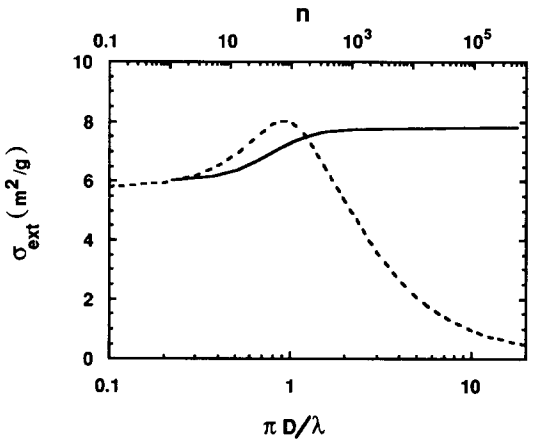

Fig. 4. Specific extinction vs number of primary particles, n for $\lambda = 630$ nm, $d_p = 45$ nm, $m = 1.55 + i0.78$, $D_f = 1.75$, $k_f = 9.0$. The dotted line is the Mie theory prediction for the volume equivalent diameter of the aggregate of n primary particles with the same value of refractive index.

The solid line shows the specific extinction increasing from the component due to absorption to a plateau that includes the increment due to scattering. The prediction of Mie theory for a sphere of the volume equivalent diameter $D = n^{1/3} d_p$ for the same wavelength and refractive index is also shown. In this case σ_{ext} decreases monotonically from its maximum near $\pi D/\lambda$ near unity. With the estimates of $\overline{n^1}$ given above we would find σ_{ext} to decrease by a factor of two if Mie theory were to be employed. Additionally, the albedo for a large partially absorbing sphere exceeds 50%. Thus, the present experiments generally support the use of the aggregate cross-sections, and they refute attempts to apply Mie theory for spheres in describing the optical behavior of filous structures.

From the decay of c_n with time a cluster–cluster aggregation rate of 15×10^{-10} cm^3 s^{-1} is calculated. This compares with a value of 8×10^{-10} cm^3 s^{-1} found in similar experiments (Colbeck *et al.*, 1989).

7. SUMMARY

A theoretical description of the specific extinction of light by randomly oriented absorbing aggregates has been presented which specifically accommodates the polydispersity resulting from cluster–cluster aggregation. Specific extinction was measured at three wavelengths of light for aging smokes over 90–120 min time intervals. Aggregate number concentrations and mass concentrations decreased as would be expected when cluster–cluster aggregation is present and when aggregates are lost by diffusion or by settling. However, the specific extinction at all three wavelengths remained essentially constant throughout the duration of the tests even though aggregate growth amounted to a factor of three in terms of volume equivalent diameter or a factor of 24 in terms of the average number of primary particles per aggregate. These results are in agreement with the theoretical prediction that specific extinction is independent of aggregate size in the large size limit ($n > n_c$). The mass extinction coefficients so measured agree with the theoretical predictions if the real part of the refractive index is near 1.55 and the imaginary part varies systematically with the wavelength of light from the violet to IR spectral regions. However, the real and imaginary portions of the refractive index are uniquely defined only when both specific extinction and specific absorption are prescribed.

There exist several claims in the literature that the volume equivalent diameter of an aggregate can be used with Mie theory to calculate the optical behavior of aggregates. This claim is refuted by the present experimental results that show specific extinction to be independent of the volume equivalent diameter of the aggregates. The results are in agreement with a model formulated in terms of fractal-like aggregates.

Acknowledgements—The authors express thanks to Mr Michael Carrier for assistance and the graphical presentations. One of us (R.A.D.) was supported by the Center for Fire Research under Grant No. NANB1D1110 and, in part, by the Army Research Office under Grant No. DAAL03-92-G-0023. Two of us (G.W.M. and N.P.B.) were supported in part by the Mineral Management Service of the U.S. Department of Interior.

REFERENCES

Benner B. A. Jr, Bryner N. P., Wise S. A., Mulholland G. W., Lao R. C. and Fingas M. F. (1990) Polycyclic aromatic hydrocarbon emissions from the combustion of crude oil on water. *Envir. Sci. Technol.* **24,** 1418–1427.

Berry M. V. and Percival I. C. (1986) Optics of fractal clusters such as smoke. *Optica Acta* **33,** 577–591.

Bohren C. F. and Huffman D. R. (1983) *Absorption and Scattering of Light by Small Particles*, p. 135. John Wiley, New York.

Bruce C. W., Stromberg T. F., Gurton K. P. and Mozer J. B. (1991) Trans-spectral absorption and scattering of electromagnetic radiation by diesel soot. *Appl. Opt.* **30,** 1537–1546.

Cashdollar K. L., Lee C. K. and Singer J. M. (1979) Three-wavelength light transmission technique to measure smoke particle size and concentration. *Appl. Opt.* **18,** 1763–1769.

Charalampopoulos T. T. and Chang H. (1991) Aggregate parameters and fractal dimension of soot using light scattering—effect of surface growth. *Combust. Flame* **87,** 89–99.

Chen H. Y., Iskander M. F. and Penner J. E. (1990) Light scattering and absorption by fractal agglomerates and coagulation of smoke aerosols. *J. Modern Opt.* **2,** 171–181.

Colbeck I., Hardman E. J. and Harrison R. M. (1989) Optical and dynamic properties of fractal clusters of carbonaceous smokes *J. Aerosol Sci.* **20,** 765–774.

Dalzell W. H. and Sarofim A. F. (1969) Optical constants of soot and their application to heat-flux calculations. *J. Heat Transfer* **91,** 100–104.

Dobbins R. A. and Megaridis C. M. (1991) Absorption and scattering of light by polydisperse aggregates. *Appl. Opt.* **30,** 4747–4754.

Janzen J. (1979) The refractive index of colloidal carbon. *J. Colloid interf. Sci.* **69,** 436–446.

Janzen J. (1980) Extinction of light by highly nonspherical strongly absorbing colloidal particles: spectrophotometric determination of volume distributions for carbon blacks. *Appl. Opt.* **19,** 2977–2985.

Japar S. M. and Szkarlat A. C. (1981) Measurement of diesel vehicle exhaust particulate using photoacoustic spectroscopy. *Combust. Sci. Technol.* **24,** 215–219.

Köylü Ü. Ö. and Faeth G. M. (1992) Structure of overfire soot in buoyant turbulent diffusion flames at long residence times. *Combust. Flame* **89,** 140–156.

Köylü Ü. Ö. and Faeth G. M. (1993) Radiation properties of flame generated soot. *J. Heat Transfer* (submitted).

Le Chatelier H. (1926) Lecon sur le Carbone. Lib. Scientifiques. H. Herman, Paris 1926. See also Schwob Y. (1979) Acetylene black: manufacture properties, and applications. *Chemistry and Physics of Carbon* (edited by Walker P. L. Jr and Thrower P. A.), Vol. 15, 109–227.

Lee S. C. and Tien C. L. (1981) Optical constants of soot in hydrocarbon flames. Eighteenth Symposium (International) on Combustion, The Combustion Institute, pp. 1149.

Megaridis C. M. and Dobbins R. A. (1990) Morphological description of flame-generated materials. *Combust. Sci. Technol.* **77,** 95–109.

Mountain R. D. and Mulholland G. W. (1988) Light scattering from simulated smoke agglomerates. *Langmuir* **4,** 1321–1326.

Mulholland G. W., Samson R. J., Mountain R. D. and Ernst M. H. (1988) Cluster size distribution for free molecular agglomeration *J. Energy Fuels* **2,** 481–486.

Nelson J. (1989a) Test of a mean field theory for the optics of fractal cluster. *J. Modern Opt.* **36,** 1031–1057.

Nelson J. R. (1989b) SRI International Private Communication, 10 February 1989.

Nishida O. and Mukohava S. (1983) Optical measurements of soot particles in a laminar diffusion flame. *Combust. Sci. Technol.* **35,** 157–173.

Patterson E. M., Duckworth R. M., Wyman C. M., Powell E. A. and Gooch J. W. (1991) Measurements of the optical properties of the smoke emissions from plastics, hydrocarbons, and other urban fuels for nuclear winter studies. *Atmospheric Environment* **25,** 2539–2552.

Puri R., Richardson T. F., Santoro R. J. and Dobbins R. A. (1993) Aerosol dynamic processes of soot aggregates in a laminar ethene diffusion flame. *Combust. Flame* **92,** 320–333.

Roessler D. M. and Faxvog F. R. (1979) Optoacoustic measurement of optical absorption in acetylene smoke. *J. Opt. Soc. Am.* **69,** 1699–1704.

Roessler D. M. and Faxvog F. R. (1980) Optical properties of agglomerated acetylene smoke particles at 0.5145 and 10.6 Microns wavelength. *J. Opt. Soc. Am.* **70,** 230–235.

Rossman R. P. and Smith W. R. (1943) Density of carbon black by helium displacement *Ind. Engng Chem.* **35,** 972–976.

Samson R. J., Mulholland G. W. and Gentry J. W. (1987) Structural analysis of soot aggregates. *Langmuir* **3,** 272–281.

Scherrer H. C., Kittelson D. B. and Dolan D. F. (1982) Light absorption measurements of diesel particulate matter. SAE Paper 810181, Society of Automotive Engineers.

Simons B. and Williams A. (1988) A shock tube investigation of the rate of soot formation for benzene, toluene, and toluene/*n*-heptane mixtures. *Comb. Flame* **71,** 219–232.

Sorensen C. M., Cai J. and Lu N. (1992a) Test of static structure factors for describing light scattering from fractal soot aggregates. *Langmuir* **8,** 2064–2069.

Sorensen C. M., Cai J. and Lu N. (1992b) Light-scattering measurements of monomer size, monomers per aggregate, and fractal dimension for soot aggregates in flames. *Appl. Opt.* **31,** 6547–6557.

Zhang H. X., Sorensen C. M., Ramer E. R., Olivier B. J. and Merkin J. F. (1988) *In situ* optical structure factor measurements of an aggregating aerosol. *Langmuir* **4,** 867–871.